PHYSICAL REVIEW B VOLUME 12, NUMBER 8 15 OCTOBER 1975

Energy bands of (100) iron thin films*

D. G. Dempsey, Leonard Kleinman, and Ed Caruthers
Department of Physics, University of Texas, Austin, Texas 78712
(Received 25 June 1975)

We have performed a tight-binding calculation of the energy bands of a 41-layer ferromagnetic (100) iron thin film. The 23-matrix element parameters (for each spin) were obtained by fitting Tawil and Callaway's bulk band calculation at a large number of points. The diagonal matrix element parameters for the surface layers were then shifted by a constant amount to make the surface charge neutral. The energy bands were calculated at 256 points in the two-dimensional Brillouin zone (BZ) and the planar and total densities of states calculated. A detailed discussion of the surface states and resonances throughout the two-dimensional BZ is given.

I. INTRODUCTION

Transition-metal surface calculations have heretofore been of two complementary but very incomplete types. Energy levels at the center of the two-dimensional Brillouin zone (2D BZ) have been calculated for thin films,[1,2] and planar densities of states have been calculated for semi-infinite crystals using an expansion containing d functions only,[3,4] i.e., completely neglecting the effects of $s-d$ hybridization. We here present a tight-binding or linear combination of atomic orbital (LCAO) calculation for a moderately thick (41-layer) ferromagnetic (100) iron film. Such calculations have heretofore proved quite successful for semiconductors.[5] The Slater-Koster[6] LCAO matrix-element parameters for s, p, and d orbitals were obtained by fitting the bulk energy-band calculation of Tawil and Callaway[7] at a large number of points in the 3D BZ and then by varying the diagonal surface-plane parameters to obtain charge neutrality at the surface of the film. The energy bands of both the majority and minority spins are calculated at 256 points in the 2D BZ. Thus this calculation overcomes the shortcomings of the earlier calculations we have mentioned.

In Sec. II we discuss the construction and diagonalization of the thin-film Hamiltonian together with the calculation of the total and planar densities of states. In Sec. III we display the thin-film energy bands along symmetry directions in the 2D BZ as we have previously done for nearly-free-electron metals.[8,9] We discuss in some detail surface states and resonances throughout the 2D BZ.

II. CONSTRUCTION OF THE HAMILTONIANS

We chose a basis set consisting of the one $4s$ function, three $4p$ functions, and five $3d$ functions. With this basis and the LCAO method of Slater and Koster,[6] two separate bulk Hamiltonians are constructed for the majority and minority spins. The Hamiltonians are further simplified by considering only two-center integrals, i.e., parameters, and by neglecting all interactions involving third or more distant neighbors. Each of the Hamiltonians is then a function only of wave vector $\vec{k}$ and the appropriate 23 parameters[10] listed in Table I.

The two sets of parameters were determined by fitting the respective energy bands calculated by Tawil and Callaway,[7] shifted downward by 0.17 Ry to obtain a better value of the work function,[11] at 48 points in the $\frac{1}{48}$ 3D BZ. All states with energies below 0.13 Ry (after the energy shift) were included in the fit. The fitting technique for obtaining the bulk parameters used a simplex minimization algorithm[12] to minimize the rms error between the fitted and calculated energy eigenvalues. The parameters obtained were further checked against a 180-point sample in the one $\frac{1}{48}$ 3D BZ. The final rms error was 3.5×10^{-3} Ry (48-point sample) with a maximum error of 0.020 Ry (228-point sample) occurring, for both spins, in a rapidly turning Δ_1 state.

For the (001) surface of bcc Fe, the unit cell is a box covering the thickness of the film and containing one atom from each layer of the film. Every other plane has one atom in the center of the two-dimensional square unit cell while the alternate planes have atoms at the cell corners. Each layer has a separate set of nine 2D Bloch basis functions yielding 369 basis functions for 41-layer film. With an odd number of layers in the film, the central plane is a reflection plane which allows one to reduce the Hamiltonian matrix from 369×369 to 186×186 and 183×183 for even and odd solutions, respectively. (One has 9 even and 9 odd basis functions for the nth and $-n$th planes taken together, while the central $n=0$ plane has six even and three odd basis functions.) The thin-film Hamiltonian matrix was diagonalized at 256 points in the 2D BZ or 45 points in the $\frac{1}{8}$ 2D BZ. Of these, 24 are symmetry points or lie along symmetry lines in the 2D BZ where the basis sets are further reduced as shown in Table II using the standard symmetry notation.[9] The two types of planes, denoted by A and B, correspond to the atoms being at the centers or corners of the 2D unit cell, respectively. The limiting of interactions to first and second

TABLE I. First- and second-neighbor Slater-Koster LCAO parameters in Ry. The last three parameters are diagonal or zeroth neighbor.

	Majority spin		Minority spin	
Parameter	1	2	1	2
$ss\sigma$	−0.10101	−0.04284	−0.09309	−0.05047
$pp\sigma$	0.21556	0.18999	0.15575	0.12920
$pp\pi$	0.03480	−0.00246	0.00037	−0.00745
$dd\sigma$	−0.05473	−0.02151	−0.05860	−0.02438
$dd\pi$	0.02366	0.00778	0.02694	0.00915
$dd\delta$	−0.00274	−0.00107	−0.00353	−0.00129
$sp\sigma$	0.14142	0.09613	0.12870	0.07958
$sd\sigma$	−0.07258	−0.02987	−0.07710	−0.02899
$pd\sigma$	0.10131	0.03738	0.09677	−0.02011
$pd\pi$	−0.01443	−0.00324	0.03638	−0.00647
ss_0	0.16375		0.22223	
pp_0	0.62488		0.50739	
dd_0	−0.45778		−0.30198	

neighbors means that basis functions separated by more than two planes do not interact and the resulting matrix is more quickly diagonalized than would otherwise be the case.

Figures 1 and 2 contain the majority- and minority-spin planar densities of states (PDS) for several planes, as well as the total densities of states (TDS). Energy meshes of 0.005 Ry for the PDS and 0.001 Ry for the TDS were used. Each energy level was given a width equal to the mesh size and contributed proportionally to its overlap into the two nearest energy intervals in the density calculation. The PDS differ from the TDS only in that they contain a factor of the sum of the coefficients squared of the basis functions on the plane for each contributing eigenfunction and have been renormalized to have the same units as the TDS, electrons per atom per Ry.

The TDS and the PDS of the interior planes are, as expected, very similar to those of Tawil and Callaway.[7] Like the calculations of Desjonquëres and Cyrot-Lackmann,[3] the surface PDS have smaller first moments than the interior PDS or the TDS. Our curves have considerably more structure than theirs. In particular, while the dip in their TDS is filled by a broad peak in their surface PDS, our surface PDS has both a broad peak and a very sharp tall (especially for the minority spins) peak just above the broad peak in energy. Although the smoothness of their curves is undoubtedly due to their method of calculation, and some of the struc-

TABLE II. Symmetrized basis functions at points of higher symmetry. The basis set depends on whether the plane has one atom at the cell center (an A plane) or four atoms at the cell corners (a B plane). The basis is chosen to make the Hamiltonian matrix real. The further use of reflection symmetry for a film with an odd number of layers will reduce the set even further on the center (A) plane.

Symmetry	A-plane functions	B-plane functions
$\bar{\Gamma}_1$	$s,\ z,\ 3z^2-r^2$	$s,\ z,\ 3z^2-r^2$
$\bar{\Gamma}_3$	x^2-y^2	x^2-y^2
$\bar{\Gamma}_4$	xy	xy
$\bar{\Gamma}_5$	$ix,\ ixz$ (or $iy,\ iyz$)	$ix,\ ixz$ (or $iy,\ iyz$)
$\bar{M}_1$	$s,\ z,\ 3z^2-r^2$	xy
$\bar{M}_2$	null on A planes	x^2-y^2
$\bar{M}_3$	x^2-y^2	null on B planes
$\bar{M}_4$	xy	$s,\ z,\ 3z^2-r^2$
$\bar{M}_5$	$ix,\ ixz$ (or $iy,\ iyz$)	$iy,\ iyz$ (or $ix,\ ixz$)
$\bar{X}_1$	$s,\ z,\ x^2-y^2,\ 3z^2-r^2$	$ix,\ ixz$
$\bar{X}_2$	xy	$iy,\ iyz$
$\bar{X}_3$	$ix,\ ixz$	$s,\ z,\ x^2-y^2,\ 3z^2-r^2$
$\bar{X}_4$	$iy,\ iyz$	xy
$\bar{\Delta}_1$	$s,\ ix,\ z,\ ixz,\ x^2-y^2,\ 3z^2-r^2$	$s,\ ix,\ z,\ ixz,\ x^2-y^2,\ 3z^2-r^2$
$\bar{\Delta}_2$	$iy,\ xy,\ iyz$	$iy,\ xy,\ iyz$
$\bar{Y}_1$	$s,\ iy,\ z,\ iyz,\ x^2-y^2,\ 3z^2-r^2$	$ix,\ xy,\ ixz$
$\bar{Y}_2$	$ix,\ xy,\ ixz$	$s,\ iy,\ z,\ iyz,\ x^2-y^2,\ 3z^2-r^2$
$\bar{\Sigma}_1$	$s,\ \frac{i}{\sqrt{2}}(x+y),\ z,\ xy,\ \frac{i}{\sqrt{2}}(xz+yz),\ 3z^2-r^2$	$s,\ \frac{i}{\sqrt{2}}(x+y),\ z,\ xy,\ \frac{i}{\sqrt{2}}(xz+yz),\ 3z^2-r^2$
$\bar{\Sigma}_2$	$\frac{i}{\sqrt{2}}(x-y),\ \frac{i}{\sqrt{2}}(xz-yz),\ x^2-y^2$	$\frac{i}{\sqrt{2}}(x-y),\ \frac{i}{\sqrt{2}}(xz-yz),\ x^2-y^2$

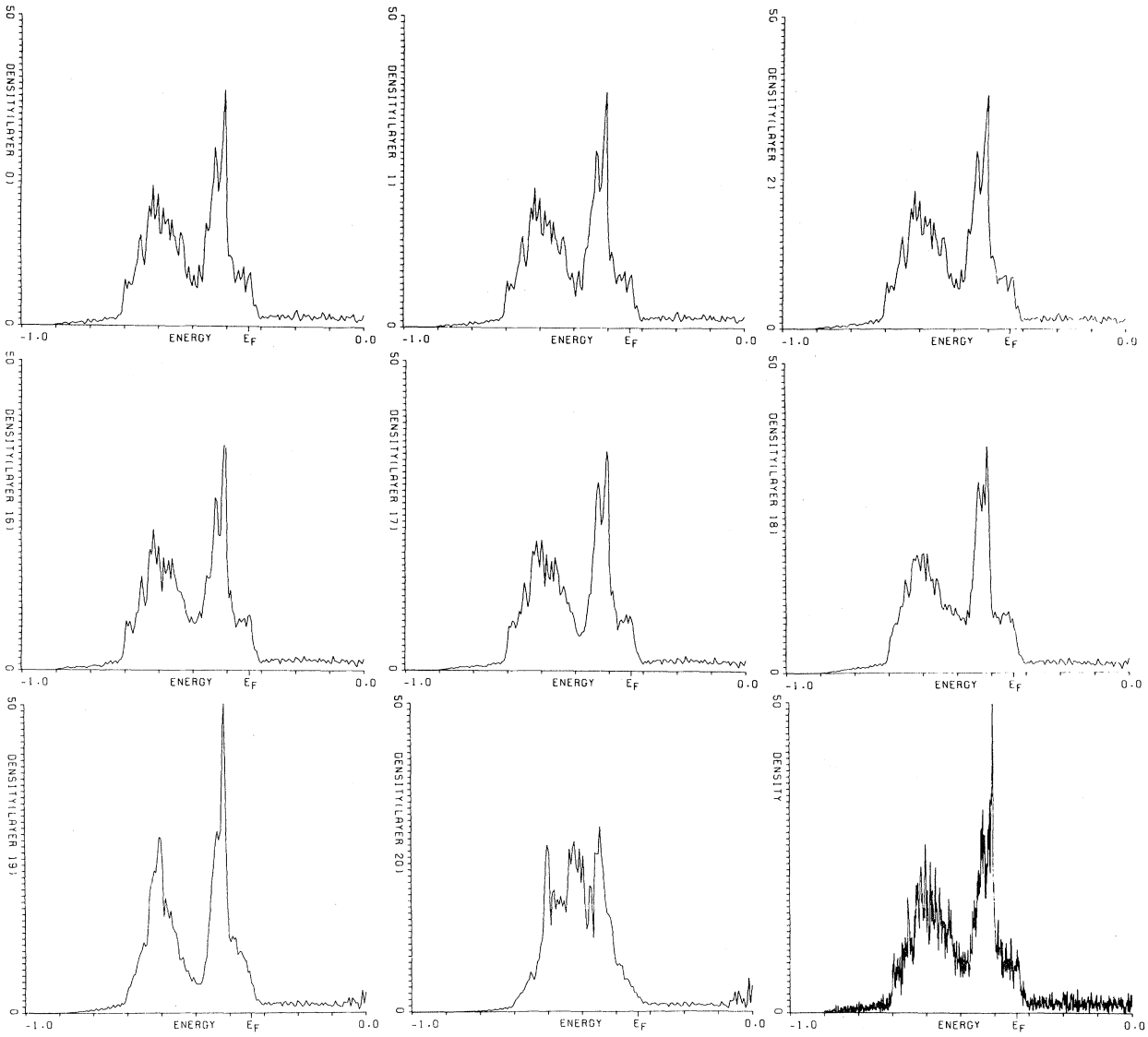

FIG. 1. Planar and total densities of states for majority spins in units of electrons per atom per Ry. Layer 0 is the central plane and 20 is the surface plane.

ture in ours is noise, their lack of this sharp peak in the surface PDS is probably due to their failure to include s and p basis functions and the resultant failure to obtain $s-d$ hybridized surface states.

While the PDS for planes beneath the surface more closely resemble the TDS than the surface PDS, their form varies as we move away from the surface and minor differences persist well into the film. Even at the film center the PDS on the A planes 0 and 2 differ slightly from the PDS on the B planes 1 and 3. This difference is most noticeable in the structure on the low-energy side of the high-energy peak.

The Fermi level was calculated by summing the TDS of both spins up to that energy which yields eight electrons per atom. In the original calculation, the number of electrons on the surface atoms, obtained by summing the surface PDS, was 7.48. We then shifted all diagonal surface parameters by -0.0217 Ry which caused an increase of 0.471 minority and 0.050 majority-spin electrons per atom, giving 8.003 electrons per surface atom. There are fluctuations away from eight as large as 0.04 electrons per atom on planes close to the surface, whereas in the interior the fluctuations do not exceed 0.01. The calculation gives essentially the same surface as total spin polarization ($5.126\uparrow$ and $2.877\downarrow$ to $5.149\uparrow$ and $2.851\downarrow$). Had we required the majority- and minority-spin diagonal surface parameters to be identical, we would have ob-

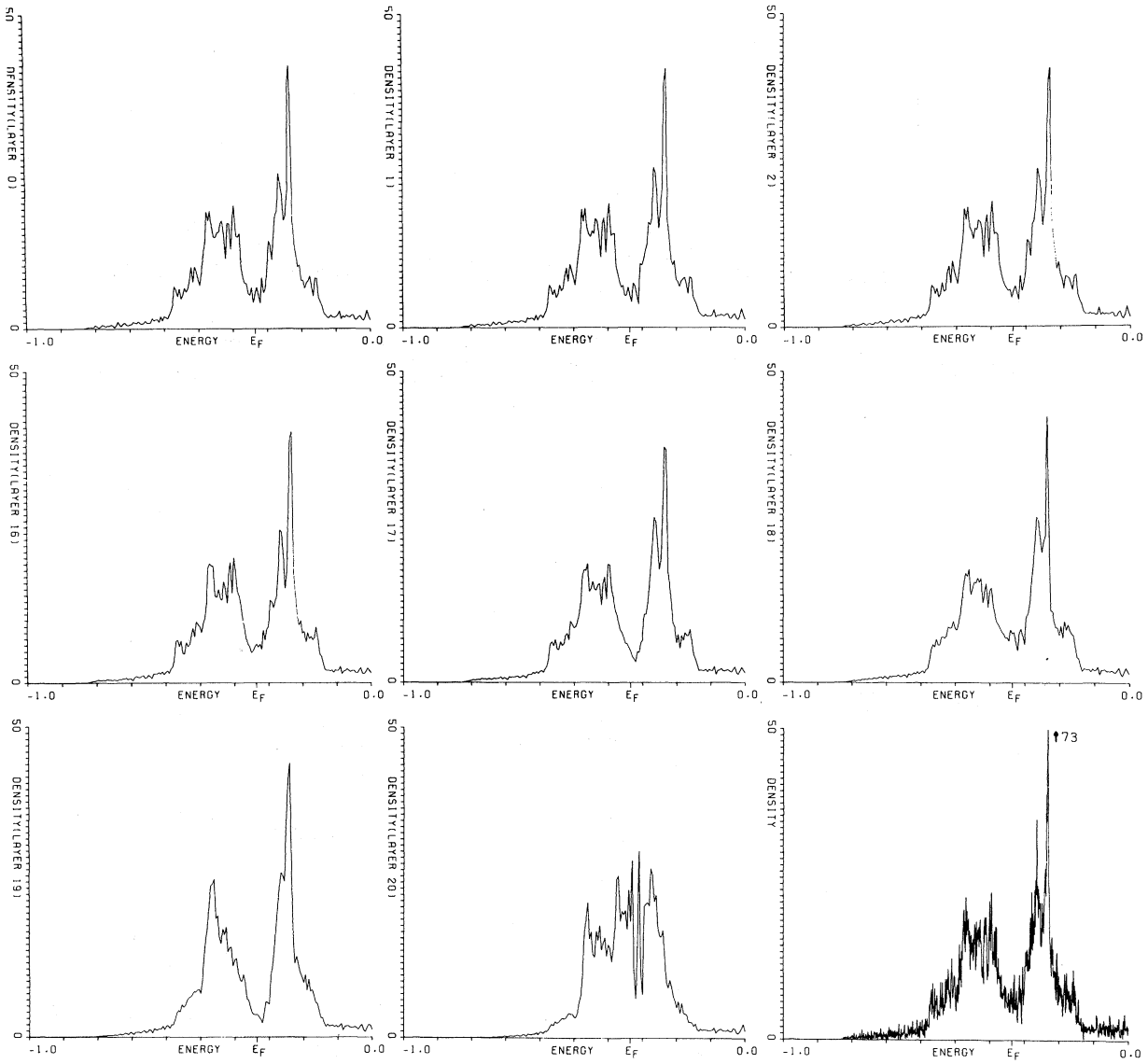

FIG. 2. Planar and total densities of states for minority spins in units of electrons per atom per Ry. Layer 0 is the central plane, and 20 is the surface plane.

tained a surface layer very nearly magnetically dead.[13]

III. ENERGY BANDS

The energy bands for each spin were calculated at 256 points in the 2D BZ using the parameters of Table I except that ss_0, pp_0, and dd_0 in the surface plane were shifted by -0.0217 Ry to make the surface plane electrically neutral. Figure 3 displays the $\bar{\Delta}_1 - \bar{Y}_1 - \bar{\Sigma}_1$ and $\bar{\Delta}_2 - \bar{Y}_2 - \bar{\Sigma}_2$ bands for the majority spin as well as the total composite $\bar{\Delta} - \bar{Y} - \bar{\Sigma}$ bands. The bands of different symmetries are separated to show the gaps and surface states which are obscured in the composite. Figure 4 depicts the corresponding energy bands for the minority-spin case. In both sets of figures, the bands at the three symmetry points are further broken down with the dots indicating the individual surface states at those points. These bands differ in form from the projected bands of Caruthers and Kleinman[14] primarily because of the differences between the ferromagnetic bulk calculation used here[7] and the paramagnetic iron calculation by Wood[15] which they used. In many cases, the minority-spin bands differ from the majority-spin bands by an upward translation of roughly 0.07 Ry. Therefore, in the following discussion, we will discuss the majority-spin band and mention the minority band's structure only if that structure, aside from the energy shift, differs significantly from the majority case.

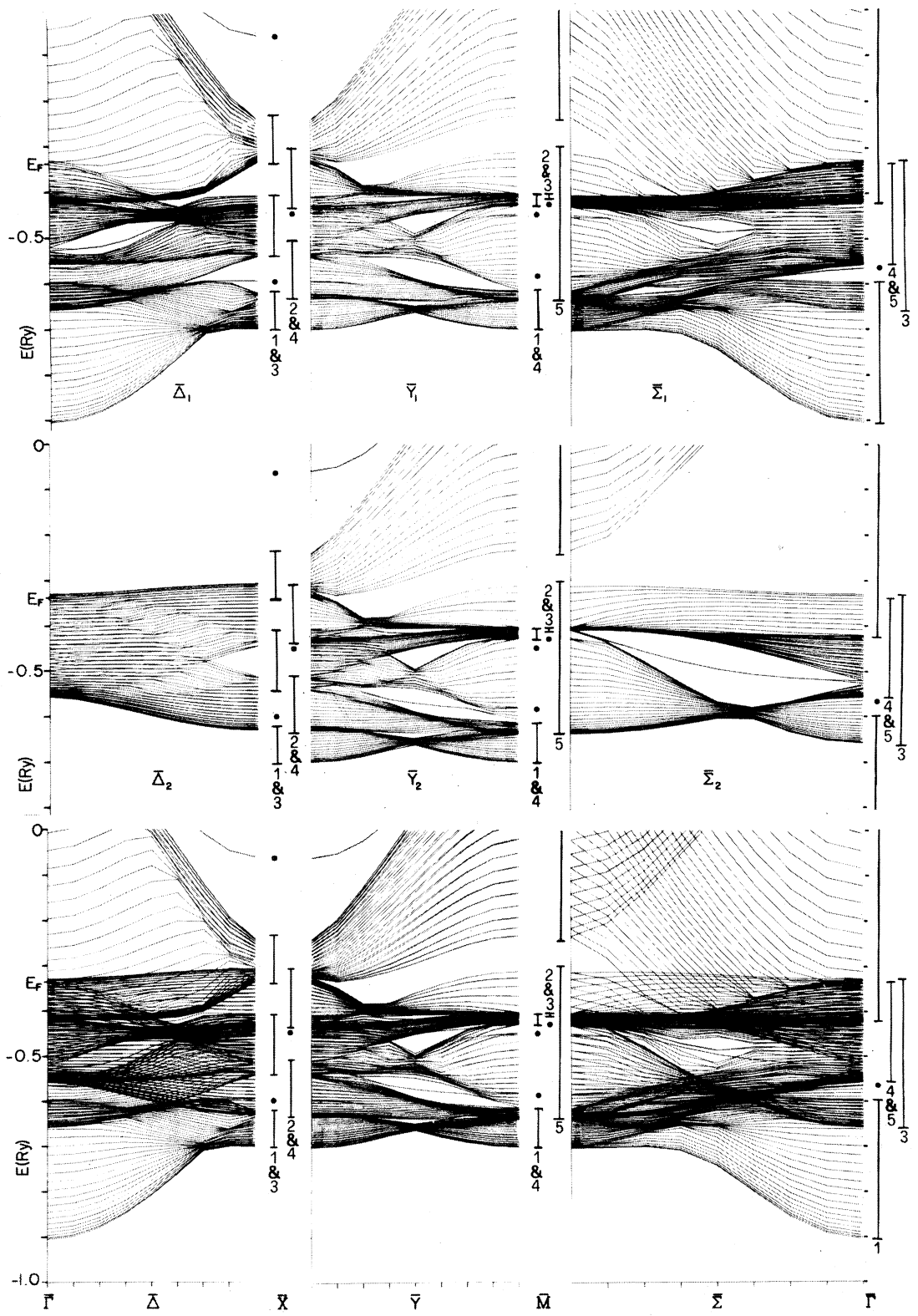

FIG. 3. Majority-spin energy bands. The symmetries of the surface states are (reading from higher to lower energy within each group) $\bar{\Gamma}_1$; $\bar{M}_3$, $\bar{M}_1$, $\bar{M}_4$; $\bar{X}_3$, $\bar{X}_4$, $\bar{X}_1$.

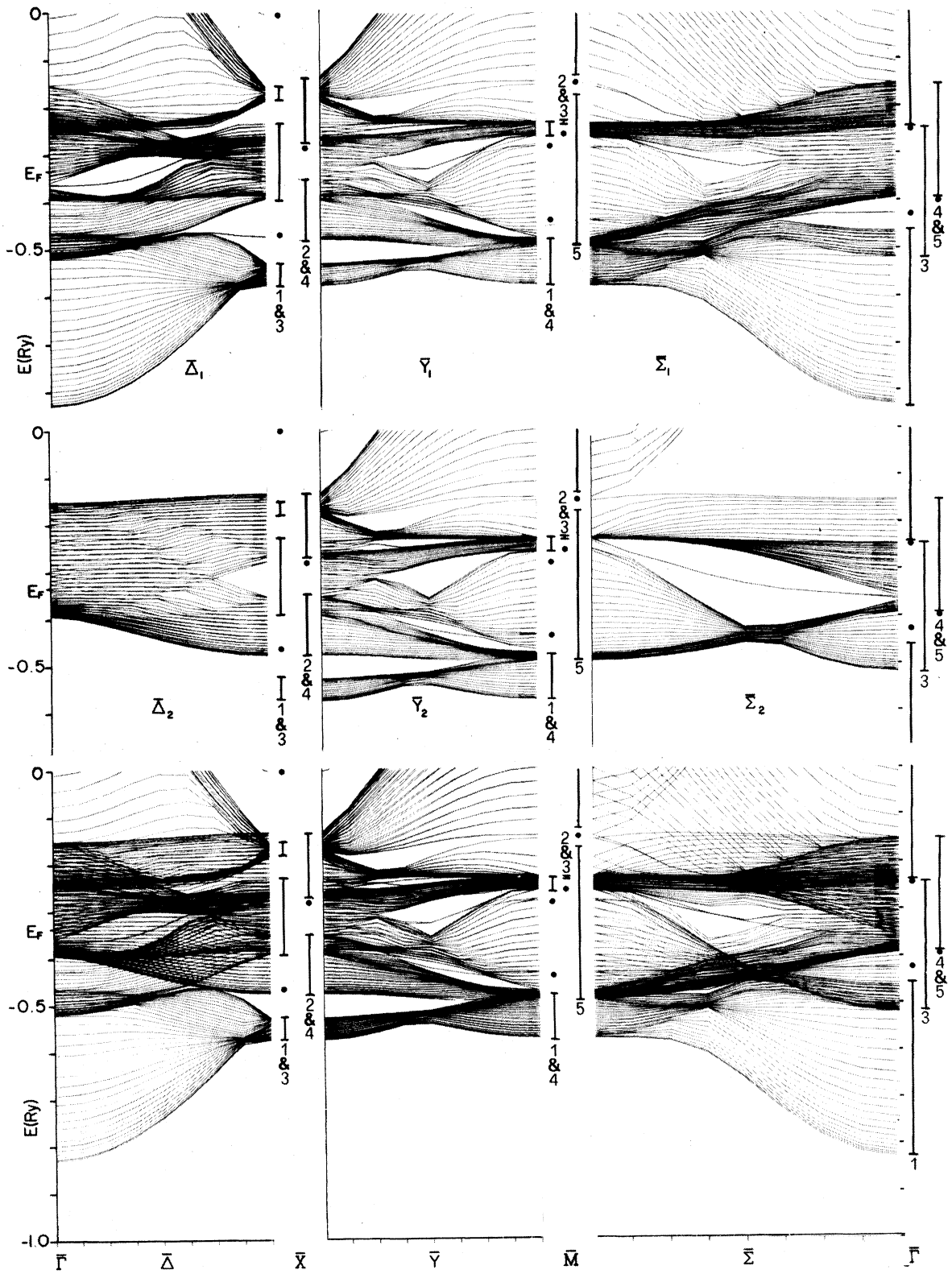

FIG. 4. Minority-spin energy bands. The symmetries of the surface states are (reading from higher to lower energy within each group) $\bar{\Gamma}_1$, $\bar{\Gamma}_5$, $\bar{\Gamma}_1$, $\bar{M}_3$, $\bar{M}_1$, $\bar{M}_4$, $\bar{X}_3$, $\bar{X}_4$, $\bar{X}_1$.

First we will discuss the energy bands and the surface states which they contain. These bands contain many more gaps and surface states than seen in materials such as aluminum[8] and lithium.[9] Because the surface states in iron are very dependent on the surface potential, their exact location, behavior, and even existence itself may change when a more exact (i.e., self-consistent) thin-film calculation is performed. Therefore, this discussion will be limited to the surface states' general locations and extents. After the general description we will single out some specifics and discuss their properties, such as decay[16] into bulk states or resonances, as being representative of the general behavior.

For the majority-spin bands the only absolute gap along $\bar{\Delta}$ occurs at $\bar{X}$ beginning at approximately -0.2 Ry and continuing up above the vacuum level. This cup-shaped gap continues around to the $\bar{Y}$ direction and contains one[17] surface state which, at the lines of higher symmetry, is either of $\bar{\Delta}_1$ or $\bar{Y}_2$ symmetry. This surface state has $\bar{X}_3$ symmetry at $\bar{X}$ and is the only surface state at a high-symmetry point ($\bar{\Gamma}$, $\bar{X}$, or $\bar{M}$) that exists, as a surface state, away from the symmetry point in all directions in the majority-spin energy bands. Figure 3 indicates four other $\bar{\Delta}_1$ gaps which vanish upon leaving the $\bar{\Delta}$ line because of the loss of symmetry. The first, near $\bar{X}$ at -0.4 Ry, runs half the length of $\bar{\Delta}_1$ and does not contain a surface state. The second, slightly lower at -0.42 Ry and to the left of the first, is very short but contains a $\bar{\Delta}_1$ surface state in its center. The next gap at -0.5 Ry extends from $\bar{\Gamma}$ to $\frac{5}{8}$ the distance to $\bar{X}$. It contains a $\bar{\Delta}_1$ surface state which runs almost the entire length of the gap. Note, however, that this surface state does not exist at $\bar{\Gamma}$ but instead decays into a bulk state just before $\bar{\Gamma}$. In a semi-infinite crystal this decay probably occurs right at $\bar{\Gamma}$. The fourth $\bar{\Delta}_1$ gap, near $\bar{X}$ at -0.6 Ry, closes off $\frac{3}{8}$ of the way to $\bar{\Gamma}$ and contains a $\bar{\Delta}_1$ surface state beginning at $\bar{X}$ with $\bar{X}_1$ symmetry and continuing along $\bar{\Delta}_1$ until it disappears into the bottom of this gap $\frac{1}{4}$ of the distance to $\bar{\Gamma}$. None of these last three $\bar{\Delta}_1$ surface states are in an absolute gap and therefore must decay into bulk or resonance states upon leaving the $\bar{\Delta}$ direction. In the $\bar{\Delta}_2$ symmetry, only one unoccupied gap reaching $\bar{X}$ at -0.5 Ry exists. The surface state in $\bar{X}_4$ at the top of this gap is very poorly defined in this 41-layer film and decays immediately into bulk states at the top of the $\bar{\Delta}_2$ gap upon leaving $\bar{X}$.

In the minority-spin bands, the $\bar{\Delta}$ absolute gap at $\bar{X}$ and -0.1 Ry and the $\bar{\Delta}_2$ gap in Fig. 4 have similar features to their majority-spin counterparts, but the $\bar{\Delta}_1$ gaps are considerably different. The first $\bar{\Delta}_1$ gap, which was unoccupied in the majority case, at $\bar{X}$ and -0.22 Ry here contains two $\bar{\Delta}_1$ surface states. The first of these surface states is in the half of the gap nearest $\bar{\Gamma}$ just below the top of the gap. The second, in the middle third of the gap's length, is barely above the gap bottom into which it eventually disappears before reaching $\bar{X}$. The small gap that was just to the left of the first $\bar{\Delta}_1$ gap in the majority case is not present in the minority-spin bands. In addition, the lowest $\bar{\Delta}_1$ gap, at $\bar{X}$ and -0.5 Ry, has doubled its width and now is an absolute gap which persists, like a knife slit, $\frac{2}{3}$ of the distance along $\bar{Y}$. In the $\bar{\Delta}_1$ portion of this gap, the $\bar{\Delta}_1$ surface state going into $\bar{X}_1$ is just above the top of the absolute gap and therefore must decay on leaving $\bar{\Delta}$. However, this state does vary in position when the surface potential is changed, and the state may move into the absolute gap when a more accurate surface potential is used. This new absolute gap does contain a surface state in $\bar{Y}_1$ which comes out of the top of the gap and persists from a point $\frac{3}{8}$ to a point $\frac{5}{8}$ the distance from $\bar{X}$ to $\bar{M}$. Since the absolute gap away from $\bar{Y}$ is quite shallow at those points, this surface state does not cover a large region of the 2D BZ.

Returning to Fig. 3 and the majority-spin bands, we note that $\bar{Y}_1$ and $\bar{Y}_2$ are degenerate aside from surface effects, and all gaps in these symmetries will be absolute gaps. The first gap, at $\bar{X}$ has already been discussed. The second gap running the entire length of $\bar{Y}$ at -0.33 Ry does not contain any surface states. This gap is a trough which pinches off $\frac{1}{8}$ of the distance along $\bar{\Sigma}$ in the $\bar{\Sigma}_1$ states. The trough remains constant in depth as we move along $\bar{Y}$ and pinches off as the gap closes at $\bar{X}$. The limits shown on this gap at $\bar{M}_5$ show the extent of the gap derived from a calculation with a 321-layer film at that point. The difference in these limits and those indicated by the bands coming into $\bar{M}$ is a result of the wide band spacing peculiar to that region of $\bar{M}$. We do not believe similar effects will exist elsewhere in these band calculations. The third $\bar{Y}$ gap is very narrow and occurs from $\frac{1}{3}$ to $\frac{2}{3}$ the way from $\bar{X}$ to $\bar{M}$ at an energy of about -0.41 Ry. At the midpoint of $\bar{Y}$, this gap extends $\frac{2}{3}$ of the distance of the $\bar{\Sigma}$ line (in the $\bar{\Delta}$ direction) before it finally pinches off. The gap contains one surface state in $\bar{Y}_1$ just below the top of the gap and a second surface state in $\bar{Y}_2$ just above the bottom of the gap. The fourth $\bar{Y}$ gap is just below the third $\bar{Y}$ gap at -0.48 Ry. It contains two $\bar{Y}_1$ surface states: one at the top on the right-hand side and one at the bottom on the left-hand side of the gap. This gap and the surface states in it extend to the center of the $\bar{\Sigma}$ line where they appear as the second absolute $\bar{\Sigma}$ gap at -0.45 Ry. The fifth $\bar{Y}$ gap extends from just off $\bar{M}$ $\frac{3}{4}$ of the distance to $\bar{X}$ at about -0.55 Ry. It contains a $\bar{Y}_1$ surface state just below the top of the gap

which disappears into the gap's top before reaching $\bar{M}$. A second $\bar{Y}_2$ surface state exists in the center half of the gap and decays into the bulk states before reaching either end. At its deepest point, in the center of $\bar{Y}$, this fifth gap and its surface states runs $\frac{1}{4}$ the distance to $\bar{\Sigma}$ before closing off. The sixth and final $\bar{Y}$ gap is at the center of $\bar{Y}$ at -0.65 Ry and contains a single $\bar{Y}_2$ surface state along the right-hand bottom portion of the gap. This gap, which does not extend an appreciable distance from $\bar{Y}$, can be considered the remanent, because of the difference in the bulk band structures, of the much larger gap in the minority bands which extends all the way to $\bar{\Delta}$ that was previously discussed.

The minority-spin $\bar{Y}$ gaps and surface states differ, aside from an energy shift and some slight changes in size, at only two points. One point, the bottom $\bar{Y}$ gap was discussed with its corresponding $\bar{\Delta}_1$ gap. The second difference occurs in the second $\bar{Y}$ gap at -0.18 Ry. In the majority case, this gap was empty. Here, a calculation on a 321-layer film at $\bar{M}_5$ shows two degenerate pairs of surface states and the gap width as indicated. We conclude that the two $\bar{Y}_1$ and $\bar{Y}_2$ bands coming into that state at $\bar{M}_5$ are surface states (although these states are large at the surface in our 41-layer film, we can not tell exactly where they become surface states), possibly as early as the beginning of the gap near $\bar{X}$. The pair of bands in the $\bar{Y}_1$ and $\bar{Y}_2$ gaps represents a single even-odd pair of surface states whose degeneracy has been split by the overlap of the surface states from the two surfaces. In fact, a calculation at $\bar{M}$ in a 321-layer film shows these states becoming degenerate and having an attenuation length of 25 layers. (We define attenuation length as that distance over which the square root of the sum of the squares of the coefficients of the basis functions of a single plane decreases to $1/e$ of its surface-plane value.) The two $\bar{M}_5$ pairs of surface states ($\bar{M}_5$ is twofold degenerate) can be written as a $\bar{\Sigma}_1$ pair and a $\bar{\Sigma}_2$ pair. The $\bar{\Sigma}_1$ pair exists in a $\bar{\Sigma}_1$ gap until the gap pinches off and the pair become bulk states or very weak resonances at a distance $\frac{3}{8}$ of the way toward $\bar{\Gamma}$. The attenuation length of this state drops from 25 layers at $\bar{M}$ to five layers $\frac{1}{8}$ of the distance toward $\bar{\Gamma}$. We have projected the bulk energy bands in order to understand what happens to the $\bar{\Sigma}_2$ gap, i.e., we have drawn the minority-spin bulk bands for the points $(2\pi/24a)(11, 11, \alpha)$ and $(2\pi/24a)(10, 10, \alpha)$. We find a gap in both cases but with a G_2 state above a G_4 state at $(2\pi/24a)(11, 11, 24)$ and the reverse at $(2\pi/24a)(10, 10, 24)$. Thus the $\bar{\Sigma}_2$ gap pinches off at some point between $\frac{1}{12}$ and $\frac{1}{8}$ of the way to $\bar{\Gamma}$ and immediately reopens getting very wide as one moves toward $\bar{\Gamma}$. The $\bar{\Sigma}_2$ surface state must disappear either at or before the pinch-off point. A 321-layer calculation $\frac{1}{8}$ of the way to $\bar{\Gamma}$ did not detect any sign of a surface state or a gap. This $\bar{\Sigma}_2$ surface-state behavior also occurs with no shift in the diagonal surface parameters and is a nice three-dimensional example of the surface states discussed by Shockley[18] in one dimension. The lower 3D band starts at $(\beta, \beta, 0)$ as a d state with a small amount of p mixed in and remains that way at intermediate points ending at G as either G_2 which is pure d or G_4 which is mixed p and d but mainly p (a lower G_4 level is mainly d). The upper band takes off from above the gap at G like a free-electron band. Thus when the gap at G separates a d band from a free-electron band, there is no surface state, but when the bands "cross," i.e., when the "d band" ends up p-like at G and the free-electron band beginning at G starts out as pure d, there is a Shockley surface state.

Returning to the majority-spin bands, we see this gap is an absolute gap. It pinches off in $\bar{\Sigma}_1$ $\frac{1}{4}$ of the way to $\bar{\Gamma}$. At that point, the states which pinch the gap off become resonances. A 321-layer calculation shows these resonance states lie in a continuum of $\bar{\Sigma}_1$ states, although this is not obvious in Fig. 3. Unlike the minority-spin case, there are no surface states of either $\bar{\Sigma}_1$ or $\bar{\Sigma}_2$ symmetry in this gap. The $\bar{\Sigma}_2$ gap does not pinch off because unlike the minority-spin case, the G_2 bulk state is always below the G_4. A second absolute $\bar{\Sigma}$ gap, at -0.5 Ry, is the continuation of the fourth $\bar{Y}$ gap previously discussed. In $\bar{\Sigma}_1$ we find four gaps of which the top two are partially absolute and have already been discussed. The third, at -0.6 Ry at $\bar{\Gamma}$ contains one surface state near its top. This surface state continues into $\bar{\Gamma}_1$ but does not exist in an absolute gap. The fourth $\bar{\Sigma}_1$ gap is located $\frac{1}{4}$ the distance from $\bar{M}$ to $\bar{\Gamma}$ and contains a single surface state just above the gap's bottom. Again this surface state must decay since the gap exists only at $\bar{\Sigma}$. At $\bar{\Sigma}_2$, in addition to the large empty upper gap already discussed, a second large gap at -0.5 Ry is occupied by a single surface state running almost the entire gap length. Except for the center portion which coincides with the second absolute $\bar{\Sigma}$ gap, this gap and surface state exists only at $\bar{\Sigma}$.

In addition to the differences around $\bar{M}_5$ already discussed, the minority $\bar{\Sigma}$ bands have an additional absolute gap over their majority-spin counterparts. Examining Fig. 4 we find the fourth $\bar{\Sigma}_1$ gap, located at -0.48 Ry and $\frac{3}{8}$ of the way from $\bar{M}$ to $\bar{\Gamma}$, is located slightly below the minority $\bar{\Sigma}_2$ bands and has become an absolute gap with one surface state which is itself just below the $\bar{\Sigma}_2$ bands. (There is only the one surface state pair; the two nearly degenerate bands above it in Fig. 4 are not surface states.) This gap extends less than $\frac{1}{8}$ the distance from $\bar{\Sigma}$ to $\bar{X}$.

The surface states in both spins are very sensitive to the -0.0217 Ry shift in the surface parame-

ters. This shift caused surface states to appear and disappear. In the majority bands, the surface state in $\bar{\Sigma}_1$ going into $\bar{\Gamma}$ appeared, while an $\bar{X}_2$ surface state vanished from the $\bar{X}_2$ gap. The major band gaps which generally contained one surface state before the change saw the original state decrease in energy, while most gaps acquired an additional surface state from the bulk states previously at the top of the gap. The $\bar{M}_3$ surface state appeared below the $\bar{M}_2$ and $\bar{M}_3$ continuum. This particular state is expected to depend heavily on the surface shift since, in our LCAO approximation, this symmetry has no basis function belonging to the layer adjacent to the surface layer. (See Table II.) This state has a very short attenuation length with the sums of the squares of the coefficients going from 0.999 on the surface to 0.001 on the next occupied layer. The minority-spin bands underwent similar changes with the addition of new $\bar{\Gamma}_1$ and $\bar{\Gamma}_5$ surface states. This sensitivity in the presence and position of the surface states emphasizes the necessity for a self-consistent procedure to determine the surface potential and charge distribution.

From examining the energy bands, the necessity of studying the entire band structure, rather than the isolated surface states at a single point such as $\bar{\Gamma}$, becomes apparent. Only one, in the majority-spin, or two, in the minority-spin surface states at the high-symmetry points persist as surface states in any general direction. The other surface states at the high-symmetry point contribute only as they decay into bulk states or resonances. The extent of this decay contribution, or the size and duration of the resonances, vary considerably. For instance, consider the $\bar{\Gamma}$ surface states in the minority-spin bands, Fig. 4. The lower $\bar{\Gamma}_1$ surface state (−0.4270 Ry) decays rapidly in the $\bar{\Delta}_1$ direction. The state is no longer distinguishable from the surrounding $\bar{\Delta}_1$ bulk states by $\frac{3}{8}$ the distance to $\bar{X}$. Along $\bar{\Sigma}_1$, this surface state does persist in a subband gap, but decays on leaving the $\bar{\Sigma}$ direction because of the loss of symmetry. The $\bar{\Gamma}_5$ surface state decays in the $\bar{\Delta}_2$ symmetry into a bulk state by $\frac{1}{8}$ of the way to $\bar{X}$. However, the $\bar{\Gamma}_5$ state, in the $\bar{\Sigma}_1$, $\bar{\Sigma}_2$, $\bar{Y}_1$, $\bar{Y}_2$, and $\bar{\Delta}_1$ symmetries, persists as a resonance around the entire 2D BZ. Thus, while the $\bar{\Gamma}_1$ surface states (at −0.4270 Ry) contributes over only 10% of the 2D BZ, the $\bar{\Gamma}_5$ state contributes over the entire 2D BZ. Because of this variable contribution and the numerous surface states in the absolute gaps, we believe any adequate study of surface states and properties must include all regions of the 2D BZ and not merely the points of highest symmetry.

In general, the decay of a surface state, whether it is due to a loss of symmetry away from a subband gap or to the closing of an absolute gap, may be quite rapid, leading to a state which is indistinguishable from the surrounding bulk, or very slow, resulting in a resonance which may spread over a large region of $\bar{k}$ space in the 2D BZ. Again, as an example, the upper $\bar{\Gamma}_1$ surface state (−0.2461 Ry) in the minority case becomes along $\bar{\Delta}_1$ a resonance of approximately the same energy until approximately $\frac{1}{2}$ the distance to $\bar{X}$. A resonance, which differs from a normal bulk state because of its eigenfunction's large surface amplitude, is not confined to a single band, as is a surface state, but jumps (or transfers the resonance properties) from band to band as it progresses in the 2D BZ. Figure 5 follows this $\bar{\Gamma}_1$ surface state along the $\bar{\Delta}_1$ line. The energy scale has been expanded and the $\bar{\Delta}_1^+$ and $\bar{\Delta}_1^-$ states are marked by + and − signs, respectively, with the $\bar{\Gamma}_1$ surface state marked as

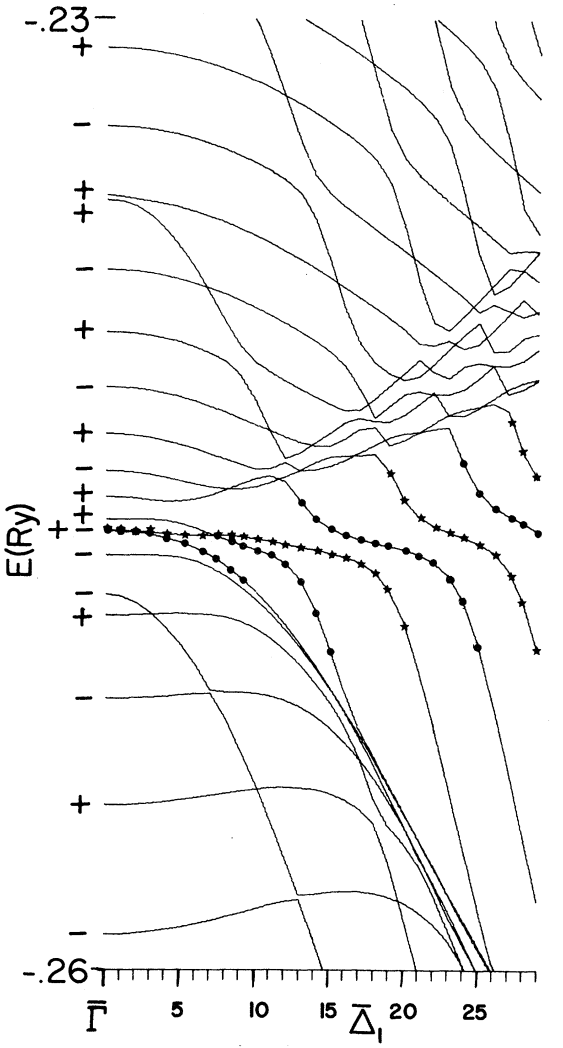

FIG. 5. Expanded view of $\bar{\Delta}_1$ minority spin energy bands showing states with resonant behavior. Stars indicate $\bar{\Delta}_1^-$ resonances and circles indicate $\bar{\Delta}_1^+$. The units of $\vec{k}$ are $(\pi/80)(1,0)$.

both, since the two are degenerate at that point. The dots denote the $\bar{\Delta}_1^+$ states which have resonance properties at that particular point, while the stars indicate the same features in the $\bar{\Delta}_1^-$ states. The resonance remains nearly constant in energy but increases in energy width as it moves away from $\bar{\Gamma}$. As the resonance state of one symmetry leaves the area of the resonance, another state of the same symmetry enters the region and acquires the resonance characteristics. Notice the resonance states in even and odd reflection symmetries are not generally degenerate. Also, unlike a surface state, the amplitude of the charge density (in our case, the sums of the squares of the coefficients) in a resonance does not attenuate to zero in the center of the film but to some relatively constant bulk value. For the resonance in Fig. 5, for example, at the $\bar{\Delta}_1$ point $(2\pi/80a, 0)$, the resonance decays to a relative amplitude squared of 0.001 in the center of the film, much like the surface state at $\bar{\Gamma}$ with the amplitude squared dropping to $1/e$ of the maximum (0.174) in two layers. Unlike the surface states whose maximum amplitude normally occurs on the surface layer, the resonances, including this one, normally peak one or two layers in from the film surface. In this case, the 0.174 peak occurs on layer 19 with surface-layer amplitude squared being only 0.069 of the total. As we move away from $\bar{\Gamma}_1$ in Fig. 5, and as the resonance moves from band to band, the resonance becomes less localized at the surface. At $(19\pi/80a, 0)$, where the $\bar{\Delta}_1^-$ resonance is switching between two bands, the amplitude squared of the lower $\bar{\Delta}_1^-$ band at the film center has increased to 0.015, while the peak amplitude on layer 19 is only 0.143 of the total. The higher-energy $\bar{\Delta}_1^-$ resonance state at this value of $\bar{k}$ is even less localized with 0.025 and 0.072 at the center and 19th layers, respectively. The attenuation length has also changed, being nearly 15 layers in this last case.

In both the majority- and minority-spin bands, two major planes of resonances extend or nearly extend throughout the 2D BZ. For the minority case (Fig. 4), the first resonance plane intersects $\bar{\Gamma}$ at -0.2461 Ry, the $\bar{\Gamma}_1$ surface state, and cuts through $\bar{\Delta}_1$ along the resonance discussed in Fig. 5 in the preceding paragraph out half way to $\bar{X}$ where the resonance breaks into several resonances above (which become a $\bar{\Delta}_1$ surface state) and below the discussed resonance. The resonance plane continues in this lower band below this $\bar{\Delta}_1$ gap and intersects $\bar{X}$ at -0.26 Ry where it appears in the $\bar{X}_1$ and $\bar{X}_3$ symmetries. The plane continues down in the $\bar{Y}_1$ and $\bar{Y}_2$ symmetry lines passing just below the second absolute $\bar{Y}$ gap and intersects $\bar{M}$ (in the $\bar{M}_1$ and $\bar{M}_4$ symmetries) with an energy of -0.23 Ry. The plane cuts across the $\bar{\Sigma}_1$ bands, with some $\bar{\Sigma}_2$ contribution near $\bar{\Gamma}$ and very near $\bar{M}$, to return to $\bar{\Gamma}$. The second plane of resonance intersects $\bar{\Gamma}_5$ at -0.39 Ry and remains nearly flat along $\bar{\Delta}$, appearing in the $\bar{\Delta}_1$ symmetries only except near $\bar{\Gamma}$, and cuts $\bar{X}_1$ and $\bar{X}_3$ at about -0.35 Ry. The plane slants down in the $\bar{Y}$ direction in both $\bar{Y}$ symmetries and passes from $\bar{X}$ just below the fifth $\bar{Y}$ gap. It intersects $\bar{M}_5$ at -0.48 Ry and slants upward along $\bar{\Sigma}$ (appearing in both $\bar{\Sigma}$ symmetries) to return to $\bar{\Gamma}_5$. The majority-spin bands in Fig. 3 possess two very similar resonance planes although the planes are shifted upward by about 0.07 Ry and the resonances on these planes are weaker, i.e., less localized in the surface regions. The extent to which these resonance are localized on the surface varies along the resonance planes and appears to be dependent on the surface potential. However, since these resonances cover the entire area of the 2D BZ, a much larger region than any of the surface states, their contribution to the surface phenomena can easily match the contributions of the surface states.

IV. SUMMARY AND CONCLUSIONS

We have presented the first calculation of thin-film transition-metal energy bands throughout the 2D BZ. We have found a wide spectrum of surface states—Shockley states and Tamm states—states with 25-layer attenuation length and with a fraction of a layer-attenuation length. An equally wide spectrum of resonances has been found—resonances which exist in only a small region of the 2D BZ and resonances which exist throughout the 2D BZ—resonances which attenuate rapidly near the surface to some fairly large bulk amplitude and resonances which attenuate more slowly but over a larger distance so that their bulk amplitude is smaller, resonances which peak on the surface plane and resonances which peak on the first or second interior planes.

Unlike the nearly-free-electron metals, the transition-metal surface states are extremely sensitive to both the surface and bulk potentials.[2] A small shift in the bulk potential can cause two states of different symmetry at some point in the 3D BZ to cross which can create or destroy a Shockley surface state, e.g., $\bar{M}_5$ in the majority- and minority-spin potentials. A shift in the surface potential creates surface states (Tamm states) and can destroy Shockley states. We believe that given a good bulk-band calculation, the tight-binding parameterization scheme does a good job on the Shockley states. The surface parameters we do not believe can be so well determined. In the first place there are 23 (or 24 considering both dd_0's[10,19]) parameters involving surface-basis functions, and we reduced this to a single shift in the three diagonal surface parameters, chosen to restore charge neutrality. In the second place, we believe the restricted tight-binding basis set to be

inadequate to describe the charge distribution in the surface region. Thus it may take an unphysical shift in the surface potential to force the inadequate basis set to yield charge neutrality. In fact, this happens in copper[20] where the density of states around the Fermi energy is much smaller than in iron, and a shift of 0.1 Ry is required to restore charge neutrality. However, when one considers the fact that other transition-metal thin-film calculations have been limited to a single layer[21] or to 20 layers[1] but only at $\bar{\Gamma}$, one begins to appreciate the utility of the parameterized LCAO calculations. When more information about surface states becomes available (either experimental or from first-principles calculations at symmetry points), the surface parameters can be adjusted to fit this data and to yield reliable results throughout the 2D BZ. The shift in the surface parameters used in this calculation can be considered to be due to a dip in the potential near the surface such as occurs in nearly-free-electron metals[9] with Friedel oscillations, and is of a reasonable magnitude. Thus the results presented here may have a considerable resemblance to reality.

ACKNOWLEDGMENT

We wish to thank Mr. Manjit Singh of Louisiana State University for providing the large sample of bulk energy eigenvalues used in obtaining the bulk parameters.

---

*Supported by National Science Foundation Grant No. DMR 73-02449-A01.

[1]R. V. Kasowski, Phys. Rev. Lett. 33, 83 (1974); and Solid State Comm. 17, 179 (1975).

[2]E. Caruthers and L. Kleinman (unpublished).

[3]M. C. Desjonqueres and F. Cyrot-Lackmann, J. Phys. (Paris) 36, L45 (1975).

[4]R. Haydock, V. Heine, and M. J. Kelly, J. Phys. C 5, 2845 (1972); and R. Haydock and M. J. Kelly, Surf. Sci. 38, 139 (1973).

[5]K. C. Pandey and J. C. Phillips, Phys. Rev. Lett. 32, 1433 (1974).

[6]J. C. Slater and G. F. Koster, Phys. Rev. 94, 1498 (1954).

[7]R. A. Tawil and J. Callaway, Phys. Rev. B 7, 4242 (1973).

[8]E. Caruthers, L. Kleinman, and G. P. Alldredge, Phys. Rev. B 8, 4570 (1973); *ibid.* 9, 3325 (1974); *ibid*; 9, 3330 (1974).

[9]G. P. Alldredge and L. Kleinman, Phys. Rev. B 10, 559 (1974).

[10]There are actually two independent dd_0 parameters, (xy/xy) and $[(3z^2-r^2)/(3z^2-r^2)]$. These were found early in the fitting operation to differ only in the third significant figure and therefore were taken to be identical to reduce the number of parameters by one.

[11]The best experimental values seem to lie between 4.5 and 4.7 eV. See A. B. Cardwell, Phys. Rev. 92, 554 (1953).

[12]J. A. Nelder and R. Mead, Comput. J. 7, 308 (1965).

[13]L. Lieberman, D. Fredkin, and H. Shore, Phys. Rev. Lett. 22, 539 (1969).

[14]E. Caruthers and L. Kleinman, Phys. Rev. B 10, 376 (1974).

[15]J. H. Wood, Phys. Rev. 126, 517 (1962).

[16]We will use the word "decay" to refer to a surface state becoming a resonance or bulk state as one moves in k space. We will refer to the "attenuation" of a surface state in real space.

[17]The surface states always occur in pairs, even and odd under reflection through the central plane. These can be combined to given surface states localized on each surface. By one surface state we mean one per surface.

[18]W. Schockley, Phys. Rev. 56, 317 (1939).

[19]In fact, because of the lack of cubic symmetry at the surface, several of the diagonal parameter degeneracies are split, e.g., the pp_0 parameter (z/z) should not be degenerate with (x/x) and (y/y).

[20]K. S. Sohn, D. G. Dempsey, L. Kleinman, and E. Caruthers (unpublished).

[21]B. R. Cooper, Phys. Rev. Lett. 30, 1316 (1973).